Data assimilation finite element method for the linearized Navier-Stokes equations in the low Reynolds regime

Muriel Boulakia, Erik Burman, Miguel Angel Fernández, Colette Voisembert

Data assimilation finite element method for the linearized Navier-Stokes equations in the low Reynolds regime

Muriel Boulakia[†,⋆], Erik Burman[‡], Miguel A. Fernández[⋆,†], and Colette Voisembert[⋆,†]

[†]Sorbonne Université & CNRS, UMR 7598 LJLL, 75005 Paris, France
[⋆]Inria Paris, 75012 Paris, France
[‡]Department of Mathematics, University College London, London WC1E 6BT, United Kingdom

October 17, 2019

Abstract

In this paper we are interested in designing and analyzing a finite element data assimilation method for laminar steady flow described by the linearized incompressible Navier-Stokes equation. We propose a weakly consistent stabilized finite element method which reconstructs the whole fluid flow from velocity measurements in a subset of the computational domain. Using the stability of the continuous problem in the form of a three balls inequality, we derive quantitative local error estimates for the velocity. Numerical simulations illustrate these convergences properties and we finally apply our method to the flow reconstruction in a blood vessel.

1 Introduction

The question of how to assimilate measured data into large scale computations of flow problems is receiving increasing attention from the computational community. There are several different situations where such data assimilation problems arise. One situation is when the data necessary to make the flow problem well posed is lacking, that is, boundary data can not be obtained on parts of the boundary, but some other measured data on the boundary or in the bulk is available to make up for this shortfall, or alternatively the position of the boundary itself is unknown. Another situation is when the initial data is unknown, but measurements are available in the (space-time) bulk domain. In such situations, the problem is ill-posed and numerical simulations are much more delicate to handle than for the well-posed flow equations. The traditional approach is to regularize the continuous problem to obtain a well-posed continuous problem, often using a variational framework, that can then be discretized using standard techniques. The regularization parameter then has to be tuned to have an optimal value with respect to noise in the data. The granularity of the computational mesh is chosen afterwards to resolve all scales of the regularized problem. An example of this strategy is the quasi-reversibility method (see the references [7, 8, 9, 10]). For examples directly related to flow problems, we refer to [9] for an application to inverse identification of boundaries subject to Stokes problem. Other examples can be found in [25], where additional measured data is used to compensate for a lack of knowledge of the boundary conditions in hemodynamics or [32] where a least squares method is proposed for combining and enhancing the results from an existing computational fluid dynamics model with experimental data.

Regardless of the application, success hinges on the existence of some stability property of the ill-posed problem. Fortunately, it is known that a relatively large class of ill-posed problems has some conditional stability property. Stability estimates give a precise information on the effect of perturbations on the system. In particular, they imply that, if the data are compatible with the PDE, in the sense that there exists a solution, in some suitable Sobolev space, satisfying both the PDE and the data, then this solution is unique. For the Stokes equation, this unique continuation property was originally proven by Fabre and Lebeau [28]. The analysis of the stability properties of ill-posed problems based on the Navier-Stokes equations is a very active field of research and we refer to the works [33, 3, 6, 31, 30, 4, 2] for recent results. Stability estimates for inverse problems classically rely on Carleman inequalities or three-balls inequalities, two tools which are strongly related. The idea of applying Carleman estimates for the stability analysis of inverse problems is introduced in the seminal paper [15] by Bukhgeim and Klibanov.

There appears to be relatively few results in the literature discussing the combined error due to regularization, discretization and perturbations for inverse problems subject to the equations of fluid mechanics. To the best of our knowledge such a combined analysis has only been performed in the recent paper [21], where a nonconforming finite element method was used, together with regularization techniques developed in the context of discontinuous Galerkin methods, to analyze a data assimilation problem for Stokes problem. One of the reasons for this is that there is in general a gap between the stability estimates that can be proven analytically and the stability required to perform a numerical analysis. An approach allowing to bridge this gap was proposed in [18, 19, 20, 22], drawing on earlier ideas for well-posed problems in [11, 12]. This framework combines stabilized finite element methods designed for well-posed problems with variational formulations for data assimilation and sharp stability estimates for the continuous problems based on three balls inequalities or Carleman estimates. Recent developments include finite element data assimilation methods with optimal error estimates for the heat equation [24, 23] and design of methods for indefinite or nonsymmetric scalar elliptic problems analyzed using Carleman estimates with explicit dependence on the physical parameters [17, 16].

In this paper, our aim is to build on these results and use known techniques for the approximation of the (well-posed) Navier-Stokes equation in an optimisation framework in order to assimilate data with computation. Contrary to the previous work [21], we consider the linearized Navier-Stokes equations and use standard H^1-conforming, piecewise affine, finite element spaces. The key idea is that the ill-posed continuous problem is not regularized. Instead, we discretize the equation and set up a constrained optimization problem where we minimize the distance between the discrete solution and the measured data. To counter the instabilities in the discrete system, we introduce weakly consistent regularization terms in such a way that the error with respect to the approximation and the underlying conditional stability is optimized. In our framework, the only regularization parameter, up to a constant scaling factor, is the mesh parameter.

The analysis is applicable to incompressible laminar steady flow in the low Reynolds regime. We are interested in a situation where a known laminar base flow U is available. A perturbation of the velocities of the base flow has been measured in some subset ω_{M} of the computational domain Ω. Assuming that the perturbation is small, we then consider a linearized equation and design a stabilized finite element method for the approximation of the global perturbation. Using a three balls inequality derived by Lin, Uhlmann and Wang [33] we derive quantitative local error estimates for the perturbations in some target subdomain ω_{T}. Herein, we only consider error estimates for local L^2-norms, but errors in local H^1-norms of velocity together with L^2-norms of pressure are also possible to analyse using three balls inequalities derived in [6], provided measurements of both velocities and pressures are available in ω_{M}.

The order of the estimate depends on the Hölder coefficient of the continuous stability estimate which depends on the size of the measure domain and the distance between the target domain and the boundary of the computational domain. For simplicity, we restrict the discussion to piecewise affine continuous approximation spaces, but the arguments can be extended to higher order finite element spaces, with the expected improvement of convergence order, following the ideas of [20]. It should however be noted that the system matrix becomes increasingly ill-posed as the polynomial order increases and the computation becomes more sensitive to noise in the measured data, so the practical interest in using high order approximation spaces remains to be proven.

The rest of the paper is organized as follows. In Section 2, we introduce the considered inverse problem and some related stability estimates. Section 3 presents the proposed stabilized finite element approximation of the data assimilation problem. The numerical analysis of the method is carried out in Section 4. Finally, Section 5 presents a series of numerical examples which illustrate the performance of the proposed method. In particular, in Section 5.3, we explore how the present approach can be applied to the estimation of relative pressure in blood flow from MRI velocity measurements.

2 Presentation of the inverse problem and stability results for the continuous problem

Let Ω be a bounded open polyhedral domain in $\mathbb{R}^d$ with $d = 2, 3$. We denote by (U, P) a solution of the stationary incompressible Navier-Stokes equations and we consider some perturbation (u, p) of this base flow. It is then known that, if the quadratic term is neglected, the linearized Navier-Stokes equations for (u, p) may be written

$$\left\{ \begin{array}{rcll} (U \cdot \nabla)u + (u \cdot \nabla)U + \nabla p - \nu \Delta u &=& f & \text{in } \Omega \\ \nabla \cdot u &=& 0 & \text{in } \Omega. \end{array} \right. \tag{1}$$

The above system is linear, but its approximation is nevertheless nontrivial, since without further assumptions on the size of ∇U, one can not prove the coercivity of the system. We assume that U belongs to $[W^{1,\infty}(\Omega)]^d$ and that the flow perturbation satisfies the regularity

$$(u, p) \in [H^2(\Omega)]^d \times H^1(\Omega).$$

In what follows, we consider that measurements on u are available in some subdomain $\omega_{\mathrm{M}} \subset \Omega$ having a nonempty interior and that these measurements are polluted by a small noise $\delta u \in [L^2(\omega_{\mathrm{M}})]^d$.

Let us now introduce some useful notations. We will consider the following spaces:

$$V := [H^1(\Omega)]^d, \quad V_0 := [H^1_0(\Omega)]^d, \quad L_0 := L^2_0(\Omega), \quad \text{and} \quad L := L^2(\Omega).$$

and the following norms, for $k = 1$ or d,

$$\|\cdot\|_L := \|\cdot\|_{[L^2(\Omega)]^k}, \; \|\cdot\|_V := \|\cdot\|_{[H^1(\Omega)]^k}, \; \|\cdot\|_{V_0'} := \|\cdot\|_{[H^{-1}(\Omega)]^d}.$$

Let us notice that, in the first two definitions, with some abuse of notation, we use the same notation for $k = 1$ and $k = d$. For any subdomain $\omega \subset \Omega$, we set

$$|v|_\omega := \left(\int_{L^2(\omega)} |v|^2 \right)^{\frac{1}{2}}, \; \forall\, v \in L^2(\omega).$$

Besides, we introduce the bilinear forms

$$a(u, v) := \int_\Omega ((U \cdot \nabla)u + (u \cdot \nabla)U) \cdot v + \nu \int_\Omega \nabla u : \nabla v, \tag{2}$$

where $H : G := \sum_{i,j=1}^{d} H_{ij} G_{ij}$ and

$$b(p, v) := \int_\Omega p \nabla \cdot v. \tag{3}$$

We will assume that the non-homogeneous linearized Navier-Stokes problem completed by homogeneous Dirichlet boundary data is well-posed:

Assumption A For all $f \in V_0'$ and $g \in L_0$, we consider the problem: find $(u, p) \in V_0 \times L_0$ such that

$$a(u, v) - b(p, v) + b(q, u) = \langle f, v \rangle_{V_0', V_0} + (g, v)_{L^2(\Omega)} \tag{4}$$

for all $(v, q) \in V_0 \times L_0$.
We assume that this problem admits a unique solution $(u, p) \in V_0 \times L_0$. Moreover, we assume that there exists $C_S > 0$ depending only on U and Ω such that, for all $f \in V_0'$ and $g \in L_0$

$$\|u\|_V + \|p\|_L \leq C_S (\|f\|_{V_0'} + \|g\|_L). \tag{5}$$

In particular, if $\|\nabla U\|_{[L^\infty(\Omega)]^{d\times d}}$ is small enough, it is straightforward to verify that Assumption A holds according to Lax-Milgram lemma. This assumption of smallness on ∇U however is a sufficient condition and there are reasons to believe that the well-posedness of system (4) holds in more general cases.

The problem that we are interested in approximating on the other hand is ill-posed. It can be expressed in the following form: $f \in V_0'$ being given, find $(u,p) \in V \times L_0$ such that

$$u = u_{\rm M} \quad \text{in} \quad \omega_{\rm M} \tag{6}$$

and

$$a(u,v) - b(p,v) + b(q,u) = \langle f, v\rangle_{V_0',V_0}, \quad \forall\,(v,q) \in V_0 \times L \tag{7}$$

Here, $u_{\rm M}$ is the measurement of the velocity made on $\omega_{\rm M}$ and we assume that $u_{\rm M}$ is given by $u_{\rm M} := u|_{\omega_{\rm M}} + \delta u$ where δu corresponds to a noise term in the velocity measurements. We observe that, compared to problem (4), the test function space has been enlarged since there are no boundary conditions on u. As a consequence, the spaces of the solution and of the test functions do not match.

In the homogeneous case, the solution (u,p) of (1) satisfies a three-balls inequality which only involves u. This result (or more precisely its non-homogeneous version given in Corollary 2.1) will be capital in the convergence study of the numerical method presented in the sequel. It is stated in [33] (with their notations, A corresponds to U and B to ∇U):

Theorem 2.1 *(Conditional stability for the linearized Navier-Stokes problem) There exists $\tilde R \in (0,1)$ such that for all $0 < R_1 < R_2 < R_3 \le R_0$ and $x_0 \in \Omega$ satisfying $R_1/R_3 < R_2/R_3 < \tilde R$ and $B_{R_0}(x_0) \subset \Omega$, we have*

$$\int_{B_{R_2}(x_0)} |u|^2 \le C \left(\int_{B_{R_3}(x_0)} |u|^2\right)^{1-\tau} \left(\int_{B_{R_1}(x_0)} |u|^2\right)^{\tau} \tag{8}$$

for $(u,p) \in [H^1(B_{R_0}(x_0))]^d \times H^1(B_{R_0}(x_0))$, solution of (1) with $f = 0$ in $B_{R_0}(x_0)$. In this inequality, C depends on R_2/R_3 and $0 < \tau < 1$ depends on R_1/R_3, R_2/R_3 and d.

To avoid the proliferation of multiplicative constants independent of the mesh size, we will frequently use the notation $a \lesssim b$ for $a \le Cb$ for some $C > 0$.

Theorem 2.1 with the help of Assumption A implies the following local stability inequality in the non-homogeneous case:

Corollary 2.1 *Let $f \in V_0'$ and $g \in L_0$ be given. For all $\omega_{\mathrm{T}} \subset\subset \Omega$, there exist $C > 0$ and $0 < \tau < 1$ such that*

$$|u|_{\omega_{\mathrm{T}}} \le C(\|f\|_{V_0'} + \|g\|_L + \|u\|_L)^{1-\tau}(\|f\|_{V_0'} + \|g\|_L + |u|_{\omega_{\mathrm{M}}})^{\tau} \tag{9}$$

for all $(u,p) \in [H^1(\Omega)]^d \times H^1(\Omega)$ solution of

$$\begin{aligned} (U\cdot\nabla)u + (u\cdot\nabla)U - \nu\Delta u + \nabla p &= f \quad \text{in } \Omega \\ \nabla\cdot u &= g \quad \text{in } \Omega. \end{aligned} \tag{10}$$

Proof: Let us first assume that there exist $x_0 \in \omega_{\mathrm{M}}$ and $0 < R_1 < R_2 < R_3 \le R_0$ such that $B_{R_1}(x_0) \subset \omega_{\mathrm{M}}$, $\omega_{\mathrm{T}} \subset B_{R_2}(x_0)$, $B_{R_0}(x_0) \subset\subset \Omega$ and $R_1/R_3 < R_2/R_3 < \tilde{R}$ where $\tilde{R}$ is defined in Theorem 2.1.

According to Assumption A, problem (4) admits a unique solution that we denote $(\tilde{u},\tilde{p}) \in V_0 \times L_0$. Then $(\tilde{w},\tilde{y}) := (u - \tilde{u}, p - \tilde{q})$ satisfies (1) with $f = 0$. Using the interior regularity of solution of Stokes problem (see for instance [35]), $(\tilde{w},\tilde{y}) \in [H^1(B_{R_0}(x_0))]^d \times H^1(B_{R_0}(x_0))$. We may then write

$$|u|_{\omega_{\mathrm{T}}} \le |\tilde{u}|_{\omega_{\mathrm{T}}} + |\tilde{w}|_{\omega_{\mathrm{T}}}.$$

For the first term in the right hand side, we use that $(\tilde{u},\tilde{p})$ satisfies the stability inequality (5):

$$|\tilde{u}|_{\omega_{\mathrm{T}}} \lesssim (\|f\|_{V_0'} + \|g\|_L).$$

For the second term, according to Theorem 2.1, $(\tilde{w},\tilde{y})$ satisfies (8) and thus:

$$|\tilde{w}|_{\omega_{\mathrm{T}}} \le \|\tilde{w}\|_{[L^2(B_{R_2}(x_0))]^d} \lesssim \|\tilde{w}\|^{1-\tau}_{[L^2(B_{R_3}(x_0))]^d}\|\tilde{w}\|^{\tau}_{[L^2(B_{R_1}(x_0))]^d} \lesssim \|\tilde{w}\|_L^{1-\tau}|\tilde{w}|^{\tau}_{\omega_{\mathrm{M}}}.$$

We now revert back to u in the right hand side:

$$\begin{aligned} |\tilde{w}|_{\omega_{\mathrm{T}}} &\lesssim (\|\tilde{u}\|_L + \|u\|_L)^{1-\tau}(|\tilde{u}|_{\omega_{\mathrm{M}}} + |u|_{\omega_{\mathrm{M}}})^{\tau} \\ &\lesssim (\|f\|_{V_0'} + \|g\|_L + \|u\|_L)^{1-\tau}(\|f\|_{V_0'} + \|g\|_L + |u|_{\omega_{\mathrm{M}}})^{\tau}. \end{aligned}$$

We conclude the proof by collecting the estimates for $\tilde{u}$ and $\tilde{w}$.

If ω_{M} and ω_{T} do not satisfy the assumptions for the construction of the balls $B_{R_1}(x_0)$ and $B_{R_0}(x_0)$, we introduce a finite sequence of intermediate balls in order to link ω_{T} to ω_{M} (as it is done for instance in [34]) and we get again the estimate. □

In a classical way for ill-posed problems [1], Corollary 2.1 gives a conditional stability result in the sense that, to be useful, this estimate has to be accompanied with an a priori bound on the solution on the global domain (due to the presence of $\|u\|_L$ in the right hand side). Let us notice that Corollary 2.1 implies in particular the uniqueness of a solution (u,p) in $[H^1(\Omega)]^d \times H^1(\Omega)$ for problem (6)-(7), up to a constant for p.

In what follows, we assume that $f \in L^2(\Omega)$ and we introduce the operator A defined on $(V \times L_0) \times (V_0 \times L)$ by

$$A[(u,p),(v,q)] := a(u,v) - b(p,v) + b(q,u) \tag{11}$$

where a and b are respectively defined by (2) and (3). Thus, we look for $(u,p) \in V \times L_0$ such that

$$A[(u,p),(v,q)] = (f,v)_{L^2(\Omega)}, \quad \forall\,(v,q) \in V_0 \times L \tag{12}$$

and (6) holds.

3 Finite element formulation

On the domain Ω, we consider a family $\{\mathcal{T}_h\}_h$ of shape regular, conforming, quasi-uniform meshes consisting of shape regular simplices K. This family is indexed by h defined as the maximum over the diameters h_K of elements in the mesh. For a fixed $h > 0$, we denote by $\mathcal{F}_i$ the set of interior faces of the mesh $\mathcal{T}_h$.

We define the jump over a face F shared by the elements K and K' (which means that $F = \bar{K} \cap \bar{K}'$) as follows: if ζ is a scalar,

$$[\![\zeta]\!]_F = \zeta|_K - \zeta|_{K'}$$

and, if ζ is a vector,

$$[\![\zeta]\!]_F = \zeta|_K \cdot n_K + \zeta|_{K'} \cdot n_{K'}$$

where n_K denotes the outward pointing normal of the element K.

We denote by X_h the standard H^1-conforming finite element space of piecewise affine functions defined on $\mathcal{T}_h$ and we introduce $V_h := [X_h]^d$, $W_h := V_h \cap V_0$, $Q_h := X_h$ and $Q_h^0 := X_h \cap L_0$.
We may then write the finite element approximation of (12): find $(u_h, p_h) \in V_h \times Q_h^0$ such that

$$A[(u_h,p_h),(v_h,q_h)] = (f,v_h)_{L^2(\Omega)}$$

for all $(v_h, q_h) \in W_h \times Q_h$. This linear system is not invertible and to regularize it, we introduce the following operators $s_u : V_h \times V_h \mapsto \mathbb{R}$, $s_u^* : W_h \times W_h \mapsto \mathbb{R}$, and for the pressure $s_p : Q_h^0 \times Q_h^0 \mapsto \mathbb{R}$ and $s_p^* : Q_h \times Q_h \mapsto \mathbb{R}$ defined by

$$\begin{aligned} s_u(u_h, v_h) &:= \gamma_u \sum_{F \in \mathcal{F}_i} \int_F h_F [\![\nabla u_h]\!] [\![\nabla v_h]\!] + \gamma_{div} \int_\Omega (\nabla \cdot u_h)(\nabla \cdot v_h), \\ s_p(p_h, q_h) &:= \gamma_p \int_\Omega h^2 \nabla p_h \cdot \nabla q_h \end{aligned}$$

and

$$s_u^*(z_h, w_h) := \gamma_u^* \int_\Omega \nabla z_h : \nabla w_h, \quad s_p^*(y_h, x_h) := \gamma_p^* \int_\Omega y_h x_h,$$

where γ_u, γ_p, γ_u^* and γ_p^* are positive user-defined parameters. Let us notice that the stabilization term s_p for the pressure of the direct problem comes from the Brezzi-Pitkäranta method [13].

For compactness, we introduce the primal and dual stabilizers: for all $(u_h, p_h), (v_h, q_h) \in V_h \times Q_h^0$

$$S[(u_h, p_h), (v_h, q_h)] = s_u(u_h, v_h) + s_p(p_h, q_h)$$

and, for all $(z_h, y_h), (w_h, x_h) \in W_h \times Q_h$

$$S^*[(z_h, y_h), (w_h, x_h)] = s_u^*(z_h, w_h) + s_p^*(y_h, x_h).$$

Finally, we introduce the measurement bi-linear form

$$m(u, v) = \gamma_M \int_{\omega_\mathrm{M}} uv,$$

where $\gamma_\mathrm{M} > 0$ is a free parameter representing the relative confidence in the measurements. We may then write the discrete Lagrangian $\mathcal{L} : (V_h \times Q_h^0) \times (W_h \times Q_h) \mapsto \mathbb{R}$ that will form the basis of our method as: for all $(u_h, p_h) \in (V_h \times Q_h^0)$ and $(z_h, y_h) \in (W_h \times Q_h)$

$$\begin{aligned} \mathcal{L}[(u_h, p_h), (z_h, y_h)] &:= \frac{1}{2} m(u_\mathrm{M} - u_h, u_\mathrm{M} - u_h) + A[(u_h, p_h), (z_h, y_h)] \\ &- (f, z_h)_{L^2(\Omega)} + \frac{1}{2} S[(u_h, p_h), (u_h, p_h)] - \frac{1}{2} S^*[(z_h, y_h), (z_h, y_h)]. \end{aligned} \quad (13)$$

If we differentiate with respect to (u_h, p_h) and (z_h, y_h), we get the following optimality system: find $(u_h, p_h) \in V_h \times Q_h^0$ and $(z_h, y_h) \in W_h \times Q_h$ such that

$$\begin{aligned} A[(u_h, p_h), (w_h, x_h)] - S^*[(z_h, y_h), (w_h, x_h)] &= (f, w_h)_{L^2(\Omega)} \\ A[(v_h, q_h), (z_h, y_h)] + S[(u_h, p_h), (v_h, q_h)] + m(u_h, v_h) &= m(u_\mathrm{M}, v_h) \end{aligned} \quad (14)$$

for all $(v_h, q_h) \in V_h \times Q_h^0$ and all $(w_h, x_h) \in W_h \times Q_h$.

We can already notice that formulation (14) is weakly consistent in the sense that we have a modified Galerkin orthogonality relation with respect to the scalar product associated to A:

Lemma 3.1 *(Consistency) Let (u, p) satisfy (1) and (u_h, p_h) be a solution of (14). Then there holds*

$$A[(u - u_h, p - p_h), (w_h, x_h)] = -S^*[(z_h, y_h), (w_h, x_h)] \tag{15}$$

for all $(w_h, x_h) \in W_h \times Q_h$.

Proof: The result is immediate by taking the difference between (12) and the first equation of (14). □

A crucial inequality to get the stability of the method is the following Poincaré inequality that we recall from [22] (Lemma 2). For all $v_h \in V_h$, we have

$$h\|v_h\|_V \lesssim (s_u(v_h, v_h) + \gamma_M |v_h|^2_{\omega_M})^{\frac{1}{2}}. \tag{16}$$

If we take in the variational formulation (14) the test functions $w_h = -z_h$, $x_h = -y_h$ and $v_h = u_h$, $q_h = p_h$ we see that, for any solution $(u_h, p_h) \in V_h \times Q_h^0, (z_h, y_h) \in W_h \times Q_h$, there holds

$$S[(u_h, p_h), (u_h, p_h)] + S^*[(z_h, y_h), (z_h, y_h)] + \gamma_M |u_h|^2_{\omega_\mathrm{M}} = -(f, z_h)_L + m(u_\mathrm{M}, u_h). \tag{17}$$

Then, according to (16), the left hand side in equation (17) is the square of a norm in $(V_h \times Q_h^0) \times (W_h \times Q_h)$ and, according to Babuska-Necas-Brezzi theorem (see [27]), we conclude that the square linear system defined by (14) admits a unique solution for all $h > 0$.

In the analysis below, we will use the following classical inverse and trace inequalities:

- Inverse inequality (see [26, Section 1.4.3]),

  $$|v|_{H^1(K)} \lesssim h_K^{-1} \|v\|_{L^2(K)} \quad \forall v \in \mathbb{P}_1(K). \tag{18}$$

  Here $\mathbb{P}_1(K)$ denotes the set of polynomials of degree less than or equal to 1 on the simplex K.

- Trace inequalities (see [26, Section 1.4.3]),

  $$\|v\|_{L^2(\partial K)} \leq C \left(h_K^{-\frac{1}{2}} \|v\|_{L^2(K)} + h_K^{\frac{1}{2}} \|v\|_{H^1(K)} \right) \quad \forall v \in H^1(K). \tag{19}$$

At last, by combining (19) and (18)

$$\|v\|_{L^2(\partial K)} \leq C h_K^{-\frac{1}{2}} \|v\|_{L^2(K)} \quad \forall v \in \mathbb{P}_1(K). \tag{20}$$

4 Stability and error analysis

Let us first define the semi-norms associated to the stabilization operators defined on $([H^2(\Omega)]^d + V_h) \times (H^1(\Omega) + Q_h)$

$$|||(v,q)||| = h\|v\|_V + S[(v,q),(v,q)]^{\frac{1}{2}}, \quad |||(v,q)|||_* = S^*[(v,q),(v,q)]^{\frac{1}{2}}.$$

We also introduce the norm

$$\|(v,q)\|_\# := \|v\|_V + \|q\|_L.$$

Let $i_h : L^2(\Omega) \mapsto X_h$ be the Scott-Zhang interpolant. We refer to [27] for the following results: for $t = 1, 2$, we have, for all $u \in H^t(\Omega)$

$$\|u - i_h u\|_\Omega + h\|\nabla(u - i_h u)\|_\Omega + h^{\frac{1}{2}} \Big(\sum_K \|u - i_h u\|^2_{\partial K}\Big)^{1/2} \le Ch^t |u|_{H^t(\Omega)} \quad (21)$$

and for all $u \in H^2(\Omega)$

$$\Big(\sum_{F \in \mathcal{F}_i} \|\nabla(u - i_h u) \cdot n\|_F^2\Big)^{1/2} \le h^{\frac{1}{2}} |u|_{H^2(\Omega)}.$$

Using the componentwise extension of i_h to vectorial functions, we deduce the approximation bounds: $\forall (v,q) \in [H^2(\Omega)]^d \times H^1(\Omega)$

$$|||(v - i_h v, q - i_h q)||| + \|(v - i_h v, q - i_h q)\|_\# \lesssim h(\|v\|_{H^2(\Omega)} + \|q\|_{H^1(\Omega)}). \quad (22)$$

The following continuity results for the bilinear form motivates the definition of the triple norms.

Lemma 4.1 *(Continuity) For all $\varsigma \in V_h + [H^2(\Omega)]^d$ and $\varpi \in Q_h + H^1(\Omega)$ there holds*

$$A[(\varsigma, \varpi), (v_h, q_h)] \lesssim \|(\varsigma, \varpi)\|_\# |||(v_h, q_h)|||_*, \quad \forall (v_h, q_h) \in W_h \times Q_h \quad (23)$$

and, for all $(v_h, q_h) \in V_h \times Q_h^0$, for all $w \in [H_0^1(\Omega)]^d$ and $y \in L^2(\Omega)$

$$A[(v_h, q_h), (w - w_h, y - y_h)] \le |||(v_h, q_h)|||(\|w\|_V + \|y\|_L) \quad (24)$$

where $(w_h, y_h) = (i_h w, i_h y)$.

Proof: The proof of (23) directly comes from the Cauchy-Schwarz inequality applied termwise in the definition (11) of A. For the second inequality (24), we set $\tilde{w} = w - w_h$ and $\tilde{y} = y - y_h$ and notice that

$$A[(v_h, q_h), (\tilde{w}, \tilde{y})] := a(v_h, \tilde{w}) - b(q_h, \tilde{w}) + b(\tilde{y}, v_h). \tag{25}$$

For the first term in the right hand side, an integration by parts in the viscous term gives, observing that $\tilde{w}|_{\partial\Omega} = 0$,

$$a(v_h, \tilde{w}) \lesssim \|U\|_{[W^{1,\infty}(\Omega)]^d} \|hv_h\|_V \|h^{-1}\tilde{w}\|_L + \frac{1}{2} \sum_{F \in \mathcal{F}_i} \int_F [\![\nabla v_h \cdot n]\!] \cdot \tilde{w} \, \mathrm{d}s.$$

Using Cauchy-Schwarz inequality with the right scaling in h, we get

$$a(v_h, \tilde{w}) \lesssim \|U\|_{[W^{1,\infty}(\Omega)]^d} \|hv_h\|_V \|h^{-1}\tilde{w}\|_L + \sum_{F \in \mathcal{F}_i} \|h^{\frac{1}{2}} [\![\nabla v_h]\!]\|_F \|h^{-\frac{1}{2}}\tilde{w}\|_F.$$

Applying the trace inequality (19), we notice that

$$\|h^{-1}\tilde{w}\|_K + \|h^{-\frac{1}{2}}\tilde{w}\|_{\partial K} \lesssim h^{-1}\|\tilde{w}\|_K + \|\nabla \tilde{w}\|_K.$$

Then, if we take the square, sum over K and use the H^1-stability inequality of i_h (21) for $t = 1$, this inequality becomes

$$\|h^{-1}\tilde{w}\|_L + \Big(\sum_{F \in \mathcal{F}_i} \|h^{-\frac{1}{2}}\tilde{w}\|_F^2 \Big)^{1/2} \lesssim \|w\|_V.$$

As a consequence

$$a(v_h, \tilde{w}) \lesssim |||(v_h, 0)||| \, \|w\|_V.$$

Similarly, for the second term in (25), an integration by parts gives

$$|b(q_h, \tilde{w})| \le \|h\nabla q_h\|_L \|h^{-1}\tilde{w}\|_L \lesssim |||(0, q_h)||| \|w\|_V.$$

Finally, the bound for the third term in (25) is immediate by the Cauchy-Schwarz inequality and the L^2-stability of i_h

$$|b(\tilde{y}, v_h)| \le \|\nabla \cdot v_h\|_L \|\tilde{y}\|_L \lesssim |||(v_h, 0)||| \, \|y\|_L.$$

Gathering these results, we get (24). □

Remark 4.1 *The augmented Lagrangian stabilization on the divergence in the operator s_u is used in the proof of Lemma 4.1 to bound in a direct way term III but it is not strictly necessary. Indeed, if y_h is chosen as the L^2-projection of y we see that for all $x_h \in Q_h$,*

$$b(\tilde{y}, v_h) = (\tilde{y}, \nabla \cdot v_h - x_h)_L$$

and recalling that

$$\inf_{x_h \in Q_h} \|\nabla \cdot v_h - x_h\|_L \lesssim \left(\sum_{F \in \mathcal{F}_i} h_F \|[\![\nabla \cdot v_h]\!]\|_F^2 \right)^{\frac{1}{2}}$$

we conclude that

$$b(\tilde{y}, v_h) \lesssim \|y\|_L \left(\sum_{F \in \mathcal{F}_i} h_F \|[\![\nabla v_h]\!]\|_F^2 \right)^{\frac{1}{2}}.$$

Hence, the stabilization of the gradient jump is sufficient to bound this term. In practice however, it can be useful to add the stabilization term on the divergence since it allows to get a stronger coercivity estimate.

Lemma 4.2 *We assume that the solution (u, p) of (12) belongs to $[H^2(\Omega)]^d \times H^1(\Omega)$ and we consider $(u_h, p_h) \in V_h \times Q_h^0$, $(z_h, y_h) \in W_h \times Q_h$ the discrete solution of (14). Then there holds*

$$|||(u - u_h, p - p_h)||| + |||(z_h, y_h)|||_* + \gamma_M^{1/2} |u - u_h|_{\omega_{\mathrm{M}}} \leq Ch(\|u\|_{[H^2(\Omega)]^d} + \|p\|_{H^1(\Omega)}) + \gamma_M^{1/2} |\delta u|_{\omega_{\mathrm{M}}}.$$

Proof: We introduce the discrete errors $\xi_h = i_h u - u_h$, $\eta_h = i_h p - p_h$. By this way, $(u - u_h, p - p_h) = (u - i_h u, p - i_h p) + (\xi_h, \eta_h)$. First we observe that

$$|||(u - u_h, p - p_h)||| + \gamma_M^{1/2} |u - u_h|_{\omega_{\mathrm{M}}} \leq |||(u - i_h u, p - i_h p)||| + \gamma_M^{1/2} |u - i_h u|_{\omega_{\mathrm{M}}} + |||(\xi_h, \eta_h)||| + \gamma_M^{1/2} |\xi_h|_{\omega_{\mathrm{M}}}.$$

Using inequalities (22) and (21) for $t = 1$, we can directly bound the first two terms in the right hand side. For the last two terms, according to inequality (16), we have

$$|||(\xi_h, \eta_h)|||^2 + \gamma_M |\xi_h|_{\omega_{\mathrm{M}}}^2 \lesssim S[(\xi_h, \eta_h), (\xi_h, \eta_h)] + \gamma_M |\xi_h|_{\omega_{\mathrm{M}}}^2.$$

To estimate the right hand side, we notice that, using the second equation of (14) with $(v_h, q_h) = (\xi_h, \eta_h)$

$$S[(\xi_h, \eta_h), (\xi_h, \eta_h)] + \gamma_M |\xi_h|^2_{\omega_{\rm M}} - A[(\xi_h, \eta_h), (z_h, y_h)] = \\ S[(i_h u, i_h p), (\xi_h, \eta_h)] + m(i_h u - u, \xi_h) - m(\delta u, \xi_h).$$

Next, according to (15) with $(w_h, x_h) = (z_h, y_h)$, we have

$$|||(z_h, y_h)|||^2_* + A[(\xi_h, \eta_h), (z_h, y_h)] = A[(i_h u - u, i_h p - p), (z_h, y_h)].$$

Thus, adding these two equalities, we get

$$S[(\xi_h, \eta_h), (\xi_h, \eta_h)] + |\xi_h|^2_{\omega_{\rm M}} + |||(z_h, y_h)|||^2_* = \underbrace{A[(i_h u - u, i_h p - p), (z_h, y_h)]}_{I} \\ + \underbrace{S[(i_h u, i_h p), (\xi_h, \eta_h)]}_{II} + \underbrace{m(i_h u - u, \xi_h) - m(\delta u, \xi_h)}_{III}.$$

We bound the terms I–III term by term. By Lemma 4.1 and the approximation bound (22), we have for term I

$$I \lesssim \|(i_h u - u, i_h p - p)\|_{\#} |||(z_h, y_h)|||_* \lesssim h(\|u\|_{[H^2(\Omega)]^d} + \|p\|_{H^1(\Omega)}) |||(z_h, y_h)|||_*.$$

For term II, we have

$$S[(i_h u, i_h p), (\xi_h, \eta_h)] = S[(i_h u - u, 0), (\xi_h, \eta_h)] + \gamma_p \int_\Omega h^2 \nabla i_h p \cdot \nabla \eta_h.$$

Thus, using (22) with $(v, q) = (u, p)$ for the first term and the H^1-stability of i_h for the second term, we get

$$II \lesssim h(\|u\|_{[H^2(\Omega)]^d} + \|p\|_{H^1(\Omega)}) |||(\xi_h, \eta_h)|||.$$

For term III, according to (21) with $t = 2$, we have

$$\begin{aligned} III &\leq \gamma_M(|i_h u - u|_{\omega_{\rm M}} + |\delta u|_{\omega_{\rm M}}) |\xi_h|_{\omega_{\rm M}} \\ &\leq (Ch^2 \|u\|_{H^2(\Omega)} + \gamma_M^{1/2} |\delta u|_{\omega_{\rm M}}) \gamma_M^{1/2} |\xi_h|_{\omega_{\rm M}}. \end{aligned}$$

Thus, collecting the above bounds, we get

$$|||(\xi_h, \eta_h)|||^2 + |||(z_h, y_h)|||^2_* + \gamma_M |\xi_h|^2_{\omega_{\rm M}} \\ \lesssim (h(\|u\|_{[H^2(\Omega)]^d} + \|p\|_{H^1(\Omega)}) + \gamma_M^{1/2} |\delta u|_{\omega_{\rm M}}) (|||(\xi_h, \eta_h)|||^2 + \gamma_M |\xi_h|^2_{\omega_{\rm M}} + |||(z_h, y_h)|||^2_*)^{\frac{1}{2}}$$

and we conclude by dividing by $(|||(\xi_h,\eta_h)|||^2 + \gamma_M^{1/2}|\xi_h|^2_{\omega_\mathrm{M}} + |||(z_h,y_h)|||^2_*)^{\frac{1}{2}}$.
□

The above lemma does not give the convergence of the error, it only asserts that some residual must converge with optimal order if the exact solution is smooth enough. Nevertheless, this lemma implies the following a priori bounds on the finite element solution.

Corollary 4.1 *Under the same assumptions as for Lemma 4.2 there holds*

$$|||(u_h,p_h)||| \lesssim h(\|u\|_{[H^2(\Omega)]^d} + \|p\|_{H^1(\Omega)}) + \gamma_M^{1/2}|\delta u|_{\omega_\mathrm{M}} \tag{26}$$

and

$$\|u_h\|_V + \|p_h\|_{H^1(\Omega)} \lesssim \|u\|_{[H^2(\Omega)]^d} + \|p\|_{H^1(\Omega)} + h^{-1}\gamma_M^{1/2}|\delta u|_{\omega_\mathrm{M}}. \tag{27}$$

Proof: In an evident way, we have

$$|||(u_h,p_h)||| \leq |||(u_h-u,p_h-p)||| + |||(u,p)|||.$$

Thus, according to Lemma 4.2 and the fact that $|||(u,p)||| = h\|u\|_V + s_p(p,p)^{\frac{1}{2}}$, we get (26). Moreover, by definition of $|||\cdot|||$, we have

$$\|u_h\|_V + \|p_h\|_{H^1(\Omega)} \lesssim h^{-1}|||(u_h,p_h)|||.$$

Thus inequality (26) directly implies (27). □

In the following theorem, we state an error estimate. The proof of this result relies on the conditional stability estimate for the continuous problem given by Corollary 2.1 and the convergence of the residual quantities given by Lemma 4.2.

Theorem 4.1 *We assume that the solution (u,p) of (12) belongs to $[H^2(\Omega)]^d \times H^1(\Omega)$ and we consider $(u_h,p_h) \in V_h \times Q_h^0$, $(z_h,y_h) \in W_h \times Q_h$ the discrete solution of (14). Then, for all $\omega_\mathrm{T} \subset\subset \Omega$, there exists $\tau \in (0,1)$ such that*

$$|u-u_h|_{\omega_\mathrm{T}} \leq Ch^\tau(\|u\|_{[H^2(\Omega)]^d} + \|p\|_{H^1(\Omega)} + h^{-1}|\delta u|_{\omega_\mathrm{M}}) + h\|f\|_L. \tag{28}$$

The constant C depends on the mesh geometry, the geometry of ω_M and ω_T and on $\|U\|_{[W^{1,\infty}(\Omega)]^{d\times d}}$.

Proof: Let us first introduce the weak formulation of the problem satisfied by $(\xi, \eta) := (u - u_h, p - p_h)$. By equation (12), we have for all $w \in V_0$ and $q \in L$,

$$A[(\xi, \eta), (w, q)] = (f, w)_{L^2(\Omega)} - A[(u_h, p_h), (w, q)]$$

We introduce, u_h and p_h being fixed, the linear forms r_f and r_g on V_0 and L respectively defined by: for all $w \in V_0$ and $q \in L$,

$$\langle r_f, w \rangle_{V_0', V_0} + (r_g, q)_L := (f, w)_{L^2(\Omega)} - A[(u_h, p_h), (w, q)].$$

It follows that (ξ, η) is solution of (10) with the functions f and g in the right hand sides replaced respectively by r_f and r_g. Applying now Corollary 2.1, we directly get

$$|\xi|_{\omega_{\mathrm{T}}} \leq C(\|r_f\|_{V_0'} + \|r_g\|_L + \|\xi\|_L)^{1-\tau}(\|r_f\|_{V_0'} + \|r_g\|_L + |\xi|_{\omega_{\mathrm{M}}})^{\tau}. \tag{29}$$

Using the first equation of (14), we can write the residuals: for all $(w_h, q_h) \in W_h \times Q_h$

$$\begin{aligned} &\langle r_f, w \rangle_{V_0', V_0} + (r_g, q)_L \\ &= (f, w - w_h)_{L^2(\Omega)} - A[(u_h, p_h), (w - w_h, q - q_h)] - S^*[(z_h, y_h), (w_h, q_h)]. \end{aligned}$$

We take $w_h = i_h w$ and $q_h = i_h q$ in this equality. For the first term, according to (21) for $t = 1$, we have

$$|(f, w - w_h)_{L^2(\Omega)}| \leq h\|f\|_L \|w\|_V.$$

The second term can be bounded by using the relations (24) and (26). For the last term, we have, according to Lemma 4.2

$$\begin{aligned} |S^*[(z_h, y_h), (w_h, q_h)]| &\leq |||(z_h, y_h)|||_* \|(w_h, q_h)\|_\# \\ &\lesssim (hC(u, p) + |\delta u|_{\omega_{\mathrm{M}}}) \|(w, q)\|_\# \end{aligned}$$

where

$$C(u, p) := \|u\|_{[H^2(\Omega)]^d} + \|p\|_{H^1(\Omega)}.$$

We thus get

$$\langle r_f, w \rangle_{V_0', V_0} + (r_g, q)_L \lesssim \big(hC(u, p) + |\delta u|_{\omega_{\mathrm{M}}} + h\|f\|_L + |||(\xi, \eta)|||\big) \|(w, q)\|_\#.$$

Since this bound holds for all $w \in V_0$ and $q \in L$, we conclude that

$$\|r_f\|_{V_0'} + \|r_g\|_L \lesssim hC(u, p) + |\delta u|_{\omega_{\mathrm{M}}} + h\|f\|_L + |||(\xi, \eta)|||.$$

Thus, we can bound the terms in the right hand side of (29) in the following way:

$$\|r_f\|_{V_0'} + \|r_g\|_L + \|\xi\|_L \lesssim C(u,p) + h\|f\|_L + h^{-1}|\delta u|_{\omega_{\rm M}}$$

according to inequalities (26) and (27) and

$$\|r_f\|_{V_0'} + \|r_g\|_L + |\xi|_{\omega_{\rm M}} \lesssim hC(u,p) + h\|f\|_L + |\delta u|_{\omega_{\rm M}}$$

according to Lemma 4.2.

Using these two bounds in (29), we conclude that

$$\begin{aligned}|\xi|_{\omega_{\rm T}} &\lesssim (C(u,p) + h^{-1}|\delta u|_{\omega_{\rm M}})^{1-\tau}(hC(u,p) + |\delta u|_{\omega_{\rm M}})^{\tau} + h\|f\|_L \\ &\lesssim h^{\tau}(C(u,p) + h^{-1}|\delta u|_{\omega_{\rm M}}) + h\|f\|_L,\end{aligned}$$

which completes the proof. □

Thus, if the measurement noise δu is equal to 0, this theorem gives the convergence of the error $u - u_h$ when h tends to 0 on any subset $\omega_{\rm T} \subset\subset \Omega$. In the case of perturbed data, the accuracy of the error is limited and inequality (28) shows that the mesh size has to balance the error due to the discretization and the error due to the noise.

5 Numerical simulations

In this section, we apply the method introduced in Section 3 in different two-dimensional different numerical examples. The free parameters in (14) are set to

$$\gamma_u = \gamma_{div} = \gamma_p = \gamma_u^* = \gamma_p^* = 10^{-1}, \quad \gamma_{\rm M} = 1000,$$

in all the numerical examples. The numerical computations have been performed with FreeFEM++ (see [29]).

5.1 Convergence study: Stokes example

In order to illustrate the convergence behavior of the method introduced in Section 3, we take up the test case presented in [21] for the Stokes system. In the unit square $\Omega = (0,1)^2$, we consider the velocity and pressure fields given by

$$u(x,y) = (20xy^3, 5x^4 - 5y^4), \quad p(x,y) = 60x^2y - 20y^3 - 5.$$

It is straightforward to verify that (u,p) is a solution to the homogeneous Stokes problem with $\nu = 1$, which corresponds to system (1) with $U = 0$

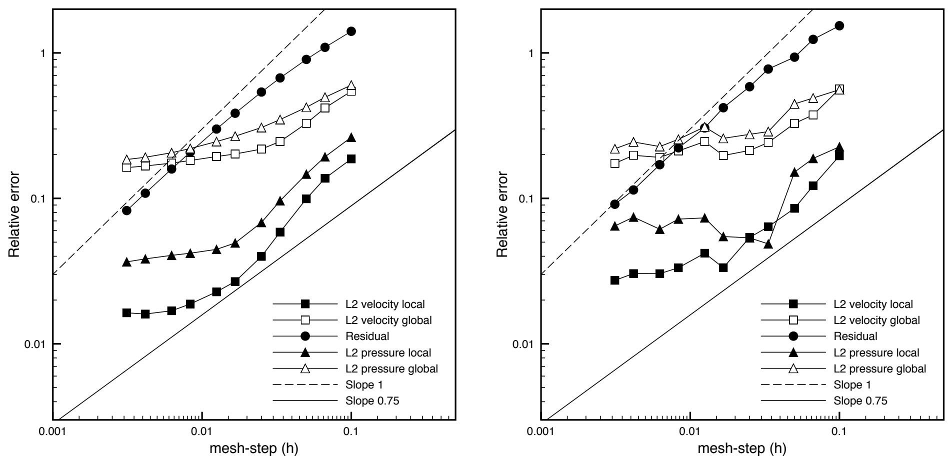

Figure 1: Relative errors against mesh size for the Stokes problem. Left: without noise. Right: with 10% noise.

and $f = 0$. We hence consider the formulation (14) with $U = 0$ and $f = 0$. The measurement and target subdomains are defined by

$$\omega_{\mathrm{M}} := (0.75, 1) \times (0.25, 0.75), \quad \omega_{\mathrm{T}} := (0.25, 1) \times (0.25, 0.75).$$

First, we perform the computation with unperturbed data. In Figure 1 (left), we report the velocity and pressure errors both in the global L^2-norm and the local L^2-norm in the subdomain ω_{T}. We also provide the convergence history of the residual quantity for the velocity stabilization:

$$\left(\sum_{F \in \mathcal{F}_i} \gamma_u \int_F \| h^{\frac{1}{2}} [\![\nabla u_h]\!] \|_{\mathcal{F}}^2 \right)^{\frac{1}{2}}.$$

The observed global asymptotic behaviors of the local velocity error (filled squares) and residual (filled circles) are in agreement with the convergence rates obtained in Theorem 4.1 and Corollary 4.1 with $|\delta u|_{\omega_{\mathrm{M}}} = 0$. It should be noted that, for the finest grids, the local velocity error tends to stagnate or increase, which can be related either to the impact of the rounding-off errors or to ill-conditioning issues of the system matrix, so that $|\delta u|_{\omega_{\mathrm{M}}} > 0$. The other error quantities, global velocity error (empty squares) and local and global pressure errors (filled and empty triangles, respectively) show a convergent behavior which also tends to stagnate for the smallest values of h. Figure 1 (right) presents the convergence history of the same quantities with a 10% Gaussian noise. The impact of the noise is clearly visible. In particular, it is worth noting that the convergence history of the local and global velocity and pressure errors is not monotone anymore and the residual loses first-order convergence rate. This is also in agreement with Theorem 4.1 and Corollary 4.1 with $|\delta u|_{\omega_{\mathrm{M}}} > 0$.

5.2 Convergence study: linearized Navier-Stokes example

In this subsection, we will use Taylor-Green vortices to construct exact solutions of (1). Let us first introduce a flow of size $R\pi$ described by a Taylor-Green vortex:

$$\begin{aligned} u_R(x,y) :=& \begin{pmatrix} -\sin(x/R)\cos(y/R)\exp(-2\nu t/R^2) \\ \cos(x/R)\sin(y/R)\exp(-2\nu t/R^2) \end{pmatrix}, \\ p_R(x,y) :=& \frac{1}{4}(\cos(2x/R)+\cos(2y/R))\exp(-4\nu t/R^2). \end{aligned}$$

For any $R > 0$, we can check that (u_R, p_R) is solution of the unsteady Navier-Stokes equations. In our numerical example, we take $\Omega = (0, 2\pi)^2$ and consider the following system which admits $(u_{\frac{1}{2}}, p_{\frac{1}{2}})$ as solution:

$$\begin{cases} (u_1\cdot\nabla)u + (u\cdot\nabla)u_1 - \nu\Delta u + \nabla p &= f \quad \text{in} \quad \Omega \\ \nabla\cdot u &= 0 \quad \text{in} \quad \Omega \end{cases}$$

where f is given by

$$f = -(u_{\frac{1}{2}}\cdot\nabla)u_{\frac{1}{2}} + (u_1\cdot\nabla)u_{\frac{1}{2}} + (u_{\frac{1}{2}}\cdot\nabla)u_1 - \partial_t u_{\frac{1}{2}}.$$

Thus, f and u_1 being given, we can use the method presented in Section 3 to reconstruct u and p from measurements on ω_{M}. The measurement and target subdomains are defined by

$$\begin{aligned} \omega_{\mathrm{M}} :=& (0,\pi/2)\times(\pi/2,3\pi/2)\cup(3\pi/2,2\pi)\times(\pi/2,3\pi/2), \\ \omega_{\mathrm{T}} :=& (\pi/2,2\pi)\times(\pi/2,3\pi/2). \end{aligned}$$

As in the previous case, we have performed numerical tests for unperturbed data and for data perturbed with a 10% noise and we have studied the convergence of the method. The obtained results are illustrated in Figure 2. The convergence curves present similarities with the ones obtained in Figure 1. We can all the same notice that, for unperturbed data, the evolution of the local velocity error is more satisfactory: it is close to the linear behavior and the error reaches much smaller values.

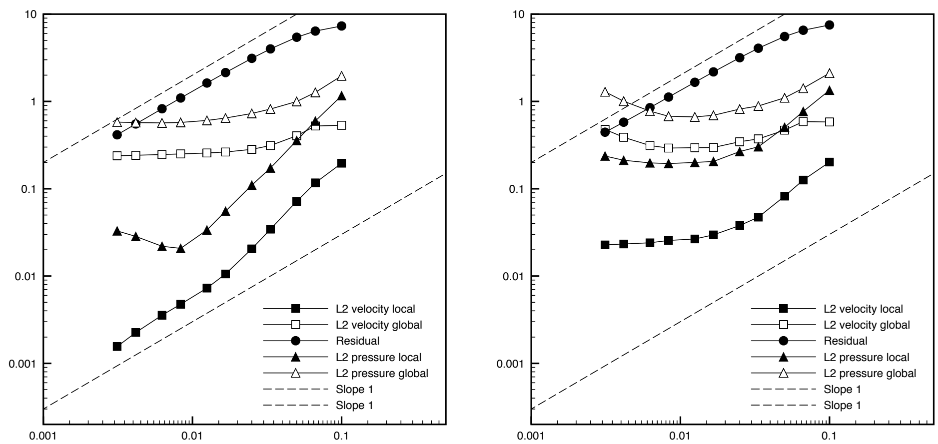

Figure 2: Relative errors against mesh size for the linearized Navier-Stokes problem. Left: without noise. Right: with 10% noise.

5.3 Application: relative blood pressure estimation from velocity measurements

To evaluate the risks related to a constriction (also called stenosis) in a blood vessel, the relative pressure difference (RPD) is a standard clinical bio-marker. Direct blood pressure measurements can however only be obtained through invasive procedures like catheterization. Non-invasive measurements are limited to the blood velocity. In particular, 4D-MRI provides a measurement of the velocity field in the whole vessel. A natural question is hence to reconstruct the RPD from these velocity measurements. We refer to [5] for a review on direct based estimation methods for this problem. The purpose of this example is to illustrate how the method introduced in Section 3 can be used to estimate the RPD from full velocity measurements.

We assume that blood flow is described by the Navier-Stokes equations and that we have velocity measurements in the whole domain Ω (see Figure 3) at a given set of time instants. We denote by $(0,T)$ the time interval, by N the number of measurements instants and set the time-step length to $\Delta t := \frac{T}{N-1}$. For all $0 \leq n \leq N-1$, the symbol u_{M}^n stands for the measured velocity at time $t_n = n\Delta t$. Then, for all $0 \leq n \leq N-2$, we consider the following Oseen type equation in terms of (u^n, p^n):

$$\begin{cases} (u_{\mathrm{M}}^n \cdot \nabla) u^n - 2\nu \nabla \cdot \varepsilon(u^n) + \nabla p^n = -\dfrac{u_{\mathrm{M}}^{n+1} - u_{\mathrm{M}}^n}{\Delta t} & \text{in} \quad \Omega, \\ \nabla \cdot u^n = 0 & \text{in} \quad \Omega. \end{cases} \tag{30}$$

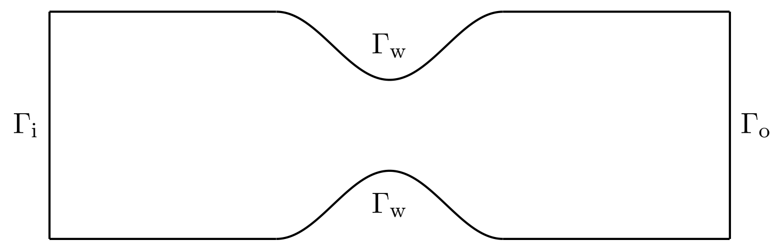

Figure 3: Geometric description of the domain Ω representing a stenotic blood vessel

Note that no boundary data is prescribed in (30), which can be cumbersome in practice since the measured velocity u_M^n is not necessarily divergence free (and hence incompatible with Dirichlet data on the whole boundary $\partial\Omega$). We hence propose to estimate u^n and p^n (up to a constant) from the data assimilation problem (12), with f and a (in the definition (11) of A) given respectively by

$$f = -\frac{u_M^{n+1} - u_M^n}{\Delta t}, \quad a(u, v) = \int_\Omega ((u_M^n \cdot \nabla)u) \cdot v + \nu \int_\Omega \varepsilon(u) : \varepsilon(v).$$

Note that, here, the measurement and target sets coincide, $\omega_M = \omega_T = \Omega$, so that the estimated velocity field u^n has to be seen as a physically driven regularization of the full velocity measure u_M^n. Yet, the main target is to estimate the RPD, defined by the following quantity:

$$\delta p = \frac{1}{|\Gamma_i|} \int_{\Gamma_i} p - \frac{1}{|\Gamma_o|} \int_{\Gamma_o} p.$$

In oder to investigate this new approach, we consider a two-dimensional version of the test case reported in [5, Section 6]. The stenotic blood vessel represented in Figure 3 corresponds to a contraction of 60%. The radii of inlet and outlet are 1 cm, the length of the vessel is 6 cm and the dynamic viscosity is given by $\nu = 0.035$ Poise. Synthetic measurements are first generated by numerically solving the incompressible Navier-Stokes system

$$\begin{cases} \partial_t u + (u \cdot \nabla)u - 2\nu \nabla \cdot \varepsilon(u) + \nabla p = 0 & \text{in} \quad \Omega \times (0, T), \\ \nabla \cdot u = 0 & \text{in} \quad \Omega \times (0, T), \end{cases} \tag{31}$$

with the following boundary and initial conditions:

$$
\begin{cases}
u = 0 & \text{on} \quad \Gamma_{\mathrm{w}} \times (0, T), \\
u = \left((-60(y^2 - 1) \sin \left(\dfrac{5\pi}{2} t \right), 0 \right) & \text{on} \quad \Gamma_{\mathrm{i}} \times (0, T), \\
2\nu\varepsilon(u)n - pn = 0 & \text{on} \quad \Gamma_{\mathrm{o}} \times (0, T), \\
u(\cdot, 0) = 0 & \text{in} \quad \Omega.
\end{cases}
\tag{32}
$$

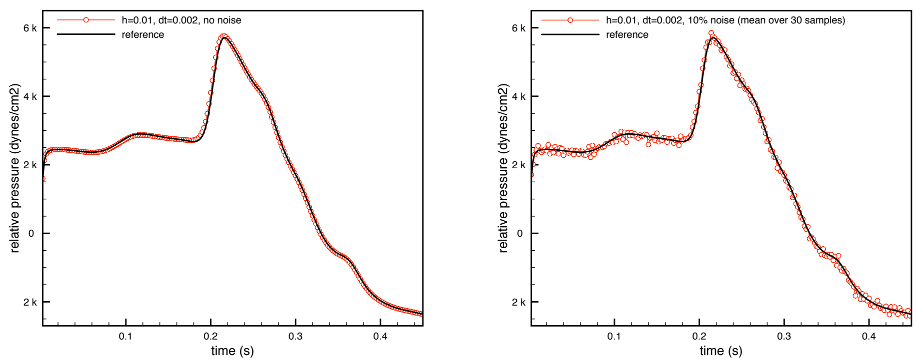

Figure 4: Left: Noise free data, right: 10% Gaussian noise on the data with exact sampling. The exact RPD is represented in full line whereas the reconstructed RPD is represented in dotted line.

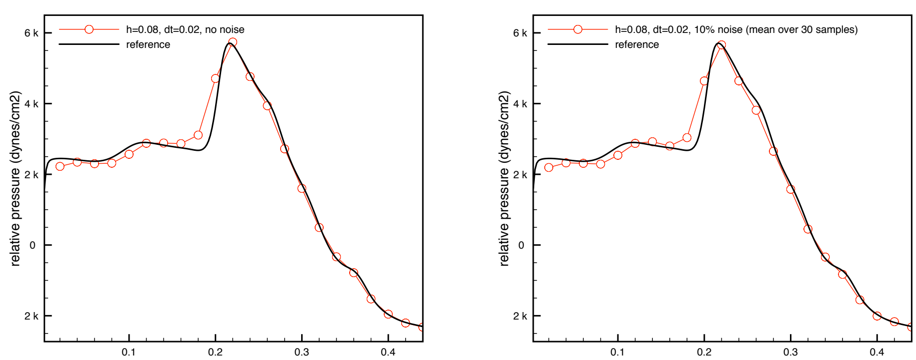

Figure 5: Left: Time subsampling of 0.02 s, right: Space subsampling of 0.08 cm. The exact RPD is represented in full line whereas the reconstructed RPD is represented in dotted line.

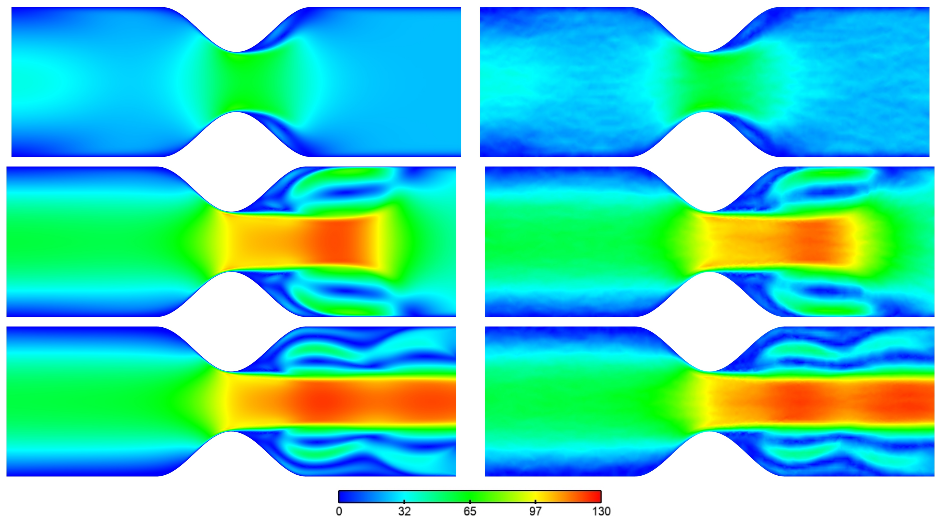

Figure 6: Velocity magnitude at $t = 0.082$, 0.162, 0.242 (from top to bottom). Right: reference. Left: reconstruction with space-time subsampling and 10% of Gaussian noise.

This direct problem (31)-(32) is discretized in space by continuous piecewise affine finite element approximations based on the SUPG/PSPG stabilization method. The time discretization consists in a backward Euler scheme with a semi-implicit treatment of the convective term. A standard backflow stabilization term is also applied on the outlet boundary Γ_o in order to guarantee the overall stability of the numerical scheme (see, e.g., [14]). The discretization parameters are set to $\Delta t = 0.002$ s and $h = 0.01$ cm. This space-time grid generates a set of synthetic velocity measurements which can be perturbed either by noise or by space-time subsampling.

Figure 4 represents the estimate RPD with the same discretization parameters as for the direct problem (no subsampling). When the data are unperturbed, we see that the reconstructed curve is perfectly superimposed with the exact curve (Figure 4, left). With a 10% Gaussian noise, we observe that the reconstructed curve (which corresponds to the mean curve obtained from 30 tests with variable noises) succeeds in following accurately the variations of the reference data (Figure 4, right).

In Figure 5, the measurements are perturbed by a subsampling both in time and in space (the time step is 10 times larger and the mesh size is 8 times larger). We then solve the data assimilation problem with the time step or the mesh size corresponding to this subsampling. Figure 5 shows that the proposed approach is able to provide a reasonable estimation of the RPD with and without noise (10% Gaussian noise). In particular, we can clearly observe that the RPD peak is well captured in both cases.

References

[1] Giovanni Alessandrini, Luca Rondi, Edi Rosset, and Sergio Vessella. The stability for the Cauchy problem for elliptic equations. *Inverse Problems*, 25(12):123004, 47, 2009.

[2] Mehdi Badra, Fabien Caubet, and Jérémi Dardé. Stability estimates for Navier-Stokes equations and application to inverse problems. *Discrete Contin. Dyn. Syst. Ser. B*, 21(8):2379–2407, 2016.

[3] Andrea Ballerini. Stable determination of an immersed body in a stationary Stokes fluid. *Inverse Problems*, 26(12):125015, 25, 2010.

[4] Mourad Bellassoued, Oleg Imanuvilov, and Masahiro Yamamoto. Carleman estimate for the Navier-Stokes equations and an application to a lateral Cauchy problem. *Inverse Problems*, 32(2):025001, 23, 2016.

[5] Cristóbal Bertoglio, Rodolfo Nuñez, Felipe Galarce, David Nordsletten, and Axel Osses. Relative pressure estimation from velocity measurements in blood flows: state-of-the-art and new approaches. *Int. J. Numer. Methods Biomed. Eng.*, 34(2):e2925, 16, 2018.

[6] Muriel Boulakia, Anne-Claire Egloffe, and Céline Grandmont. Stability estimates for the unique continuation property of the Stokes system and for an inverse boundary coefficient problem. *Inverse Problems*, 29(11):115001, 21, 2013.

[7] L. Bourgeois. A mixed formulation of quasi-reversibility to solve the Cauchy problem for Laplace's equation. *Inverse Problems*, 21(3):1087–1104, 2005.

[8] Laurent Bourgeois and Jérémi Dardé. A quasi-reversibility approach to solve the inverse obstacle problem. *Inverse Probl. Imaging*, 4(3):351–377, 2010.

[9] Laurent Bourgeois and Jérémi Dardé. The "exterior approach" to solve the inverse obstacle problem for the Stokes system. *Inverse Probl. Imaging*, 8(1):23–51, 2014.

[10] Laurent Bourgeois and Arnaud Recoquillay. A mixed formulation of the Tikhonov regularization and its application to inverse PDE problems. *ESAIM Math. Model. Numer. Anal.*, 52(1):123–145, 2018.

[11] James H. Bramble, Raytcho D. Lazarov, and Joseph E. Pasciak. A least-squares approach based on a discrete minus one inner product for first order systems. *Math. Comp.*, 66(219):935–955, 1997.

[12] James H. Bramble, Raytcho D. Lazarov, and Joseph E. Pasciak. Least-squares for second-order elliptic problems. *Comput. Methods Appl. Mech. Engrg.*, 152(1-2):195–210, 1998. Symposium on Advances in Computational Mechanics, Vol. 5 (Austin, TX, 1997).

[13] F. Brezzi and J. Pitkäranta. On the stabilization of finite element approximations of the Stokes equations. In *Efficient solutions of elliptic systems (Kiel, 1984)*, volume 10 of *Notes Numer. Fluid Mech.*, pages 11–19. Friedr. Vieweg, Braunschweig, 1984.

[14] Ch.-H. Bruneau and P. Fabrie. Effective downstream boundary conditions for incompressible navierstokes equations. *International Journal for Numerical Methods in Fluids*, 19(8):693–705, 1994.

[15] A. L. Bukhgeim and M. V. Klibanov. Uniqueness in the large of a class of multidimensional inverse problems. *Dokl. Akad. Nauk SSSR*, 260(2):269–272, 1981.

[16] E. Burman, M. Nechita, and L. Oksanen. A stabilized finite element method for inverse problems subject to the convection–diffusion equation. Part 1: Diffusion dominated refime. in preparation 2018.

[17] E. Burman, M. Nechita, and L. Oksanen. Unique continuation for the Helmholtz equation using stabilized finite element methods. *ArXiv e-prints*, October 2017.

[18] Erik Burman. Stabilized finite element methods for nonsymmetric, noncoercive, and ill-posed problems. Part I: Elliptic equations. *SIAM J. Sci. Comput.*, 35(6):A2752–A2780, 2013.

[19] Erik Burman. Error estimates for stabilized finite element methods applied to ill-posed problems. *C. R. Math. Acad. Sci. Paris*, 352(7-8):655–659, 2014.

[20] Erik Burman. Stabilised finite element methods for ill-posed problems with conditional stability. In *Building bridges: connections and challenges in modern approaches to numerical partial differential equations*, volume 114 of *Lect. Notes Comput. Sci. Eng.*, pages 93–127. Springer, [Cham], 2016.

[21] Erik Burman and Peter Hansbo. Stabilized nonconforming finite element methods for data assimilation in incompressible flows. *Math. Comp.*, 87(311):1029–1050, 2018.

[22] Erik Burman, Peter Hansbo, and Mats G. Larson. Solving ill-posed control problems by stabilized finite element methods: an alternative to Tikhonov regularization. *Inverse Problems*, 34(3):035004, 36, 2018.

[23] Erik Burman, Jonathan Ish-Horowicz, and Lauri Oksanen. Fully discrete finite element data assimilation method for the heat equation. *ESAIM: M2AN*, 2018.

[24] Erik Burman and Lauri Oksanen. Data assimilation for the heat equation using stabilized finite element methods. *Numer. Math.*, 2018.

[25] Marta D'Elia and Alessandro Veneziani. Uncertainty quantification for data assimilation in a steady incompressible Navier-Stokes problem. *ESAIM Math. Model. Numer. Anal.*, 47(4):1037–1057, 2013.

[26] Daniele Antonio Di Pietro and Alexandre Ern. *Mathematical aspects of discontinuous Galerkin methods*, volume 69 of *Mathématiques & Applications (Berlin) [Mathematics & Applications]*. Springer, Heidelberg, 2012.

[27] Alexandre Ern and Jean-Luc Guermond. *Theory and practice of finite elements*, volume 159 of *Applied Mathematical Sciences*. Springer-Verlag, New York, 2004.

[28] Caroline Fabre and Gilles Lebeau. Prolongement unique des solutions de l'equation de Stokes. *Comm. Partial Differential Equations*, 21(3-4):573–596, 1996.

[29] F. Hecht. New development in FreeFem++. *J. Numer. Math.*, 20(3-4):251–265, 2012.

[30] O. Yu. Imanuvilov and M. Yamamoto. Global uniqueness in inverse boundary value problems for the Navier-Stokes equations and Lamé system in two dimensions. *Inverse Problems*, 31(3):035004, 46, 2015.

[31] O. Yu. Imanuvilov and M. Yamamoto. Remark on boundary data for inverse boundary value problems for the Navier-Stokes equations [Addendum to MR3319370]. *Inverse Problems*, 31(10):109401, 4, 2015.

[32] Rajaraman Prathish K., Manteuffel T. A., Belohlavek M., and Heys Jeffrey J. Combining existing numerical models with data assimilation using weighted least squares finite element methods. *International Journal for Numerical Methods in Biomedical Engineering*, 33(1):e02783, 2017. e02783 CNM-Oct-15-0192.R1.

[33] Ching-Lung Lin, Gunther Uhlmann, and Jenn-Nan Wang. Optimal three-ball inequalities and quantitative uniqueness for the Stokes system. *Discrete Contin. Dyn. Syst.*, 28(3):1273–1290, 2010.

[34] Luc Robbiano. Théorème d'unicité adapté au contrôle des solutions des problèmes hyperboliques. *Comm. Partial Differential Equations*, 16(4-5):789–800, 1991.

[35] Gregory Seregin. *Lecture notes on regularity theory for the Navier-Stokes equations.* World Scientific Publishing Co. Pte. Ltd., Hackensack, NJ, 2015.